Report 15, 1993

NATURAL STATE SIMULATION OF THE MAHANAGDONG GEOTHERMAL SECTOR, LEYTE, PHILIPPINES

Nemesto Noel A. Urmeneta,
UNU Geothermal Training Programme,
Orkustofnun - National Energy Authority,
Grensasvegur 9,
108 Reykjavik,
ICELAND

Permanent address:
Reservoir Engineering and Resource Management,
Geothermal Division,
PNOC - Energy Development Corporation,
PNPC Complex, Merritt Road, Ft. Bonifacio,
Makati, Metro Manila,
PHILIPPINES

ABSTRACT

A new conceptual model for the Mahanagdong sector of the Greater Tongonan geothermal field is presented. Such a revision was partly based on the information from the latest wells drilled in the area, MG-1RD and MG-8D. The conceptual model was then translated into a three-dimensional numerical model for simulation purposes. The simulation code TOUGH was used to run the model until a near steady state condition was achieved. The model was able to duplicate the probable hydrological flow in the system. Likewise, the simulated temperatures and pressures in the wells reasonably matched the measured ones. The horizontal permeabilities were estimated to range between 0.01 - 5 mD while the vertical permeabilities range from 0.01 - 8 mD. The natural recharge is estimated to be 20 kg/s. The model, in order to be useful for exploitation simulation runs, has to be calibrated further against ample production data.

TABLE OF CONTENTS

LIST OF FIGURES

LIST OF TABLES

1. INTRODUCTION

The Mahanagdong geothermal sector is situated within the Greater Tongonan geothermal field (GTGF) in the island of Leyte, Philippines (Figure 1). The first well drilled in the sector is MG-1 which was spudded on the 11th of July 1980 by the Philippine National Oil Company - Energy Development Corporation (PNOC-EDC). At present a total of 7 production wells and 1 reinjection well has been drilled to delineate the extent of the resource.

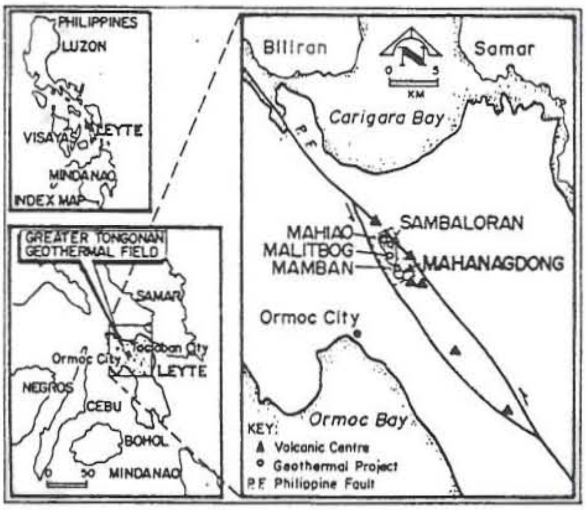

FIGURE 1: Location map, Mahanagdong geothermal sector (Bayrante et al., 1992)

A preliminary resource assessment of the Mahanagdong sector indicated that 1988-2718 MW_e-years of stored heat could be recovered as electrical energy (PNOC-EDC, 1990). Recently, PNOC-EDC made a reassessment of the geothermal resources in Leyte in line with the plan of exporting electricity to the islands of Luzon and Cebu by the year 1997 via submarine cables. The integrated resource assessment of the GTGF indicated that it has a recoverable stored heat of 11925-16775 MW_e-years (Gonzalez et al., 1993) of which the Mahanagdong sector contributes about 2675-4175 MW_e-years of energy (Bayrante et al., 1992). Based on a 25 year plant life this translates to a power potential of 107-167 MW_e. Hence, the Mahanagdong sector is being developed to produce 165 MW_e for the Leyte-Luzon interconnection.

Numerical modelling and simulation studies on the Mahiao-Sambaloran-Malitbog sector of the GTGF were carried out to predict the performance of the field under exploitation (Aunzo et al., 1986; Salera and O'Sullivan, 1987). At that time no numerical modelling and simulation studies were done on the Mahanagdong sector of the GTGF. This was not critical since Mahanagdong is considered to belong to another major upflow zone in the GTGF. To complete the picture, a study was done by Malate (Gonzalez et al., 1993) using the MULKOM simulator code which was developed at the Lawrence Berkeley Laboratory (Pruess, 1983). It utilized a two-dimensional model to simulate the natural state of the system and its behaviour under exploitation for 25 years. The simulation predicts that the reservoir could support the planned extraction of 4125 MW_e-years of electrical energy and would entail the drilling of 38 make-up and replacement wells. The results are preliminary in the sense that a two-dimensional model does not consider lateral mass and heat flow which may play a significant role during production simulation.

A three-dimensional model of the Mahanagdong sector is developed in this study to improve the current two-dimensional model of the system. Limited amount of time and production data does not warrant production simulation runs so this study is limited to the simulation of the natural state evolution of the system using the simulator code TOUGH. The results of this study will set the background for further reservoir modelling studies on the Mahanagdong sector.

2. WELL AND FLUID CHARACTERISTICS

At present there are 8 wells drilled in the sector (Figure 2) of which one well, MG-1RD, is intended as a reinjection well. In characterizing the wells two physical parameters are primarily considered, temperature and pressure. Aside from these two the injectivity, transmissivity, massflow and enthalpy of the wells were likewise utilized. The characteristics of the fluids produced by the wells are discussed under the section on fluid chemistry. The information as regards to well MG-1, MG-2D, MG-3D, MG-4D, MG-5D and MG-7D's fluid chemistry, completion test results and output characteristics were based on the resource assessment reports (PNOC-EDC, 1991; Gonzalez et al., 1993).

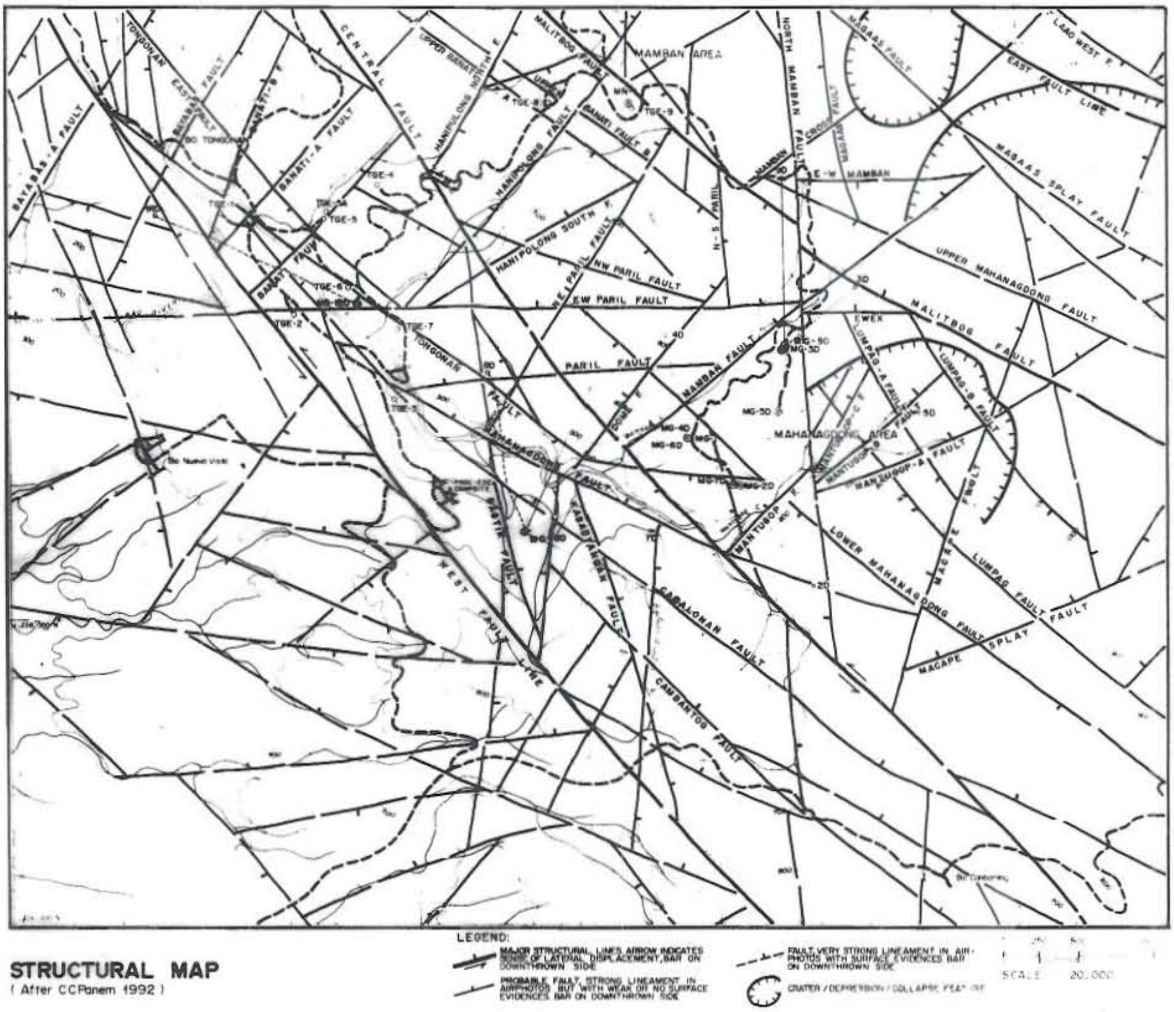

FIGURE 2: Structural map, Greater Tongonan geothermal field

2.1 Well characteristics

2.1.1 Well MG-1

Well MG-1 is the first well to be drilled within the Mahanagdong sector and so far it is the only vertical well in the area. Completion tests indicated that the well has an injectivity of 23 l/s-MPa and a transmissivity of about 3.5 Dm. Analysis of the waterloss and heat-up surveys indicate that the main permeable horizons are located at around -618 m and -1718 m a.m.s.l. During the heat-up period, pressure surveys indicate that the pivot or pressure control point (PCP) is at -718 m a.m.s.l. and the pressure at that point is 8 MPa-g (Figure 3). This indicates that the more permeable zone is the upper one. The water level is located at around 280 m a.m.s.l.

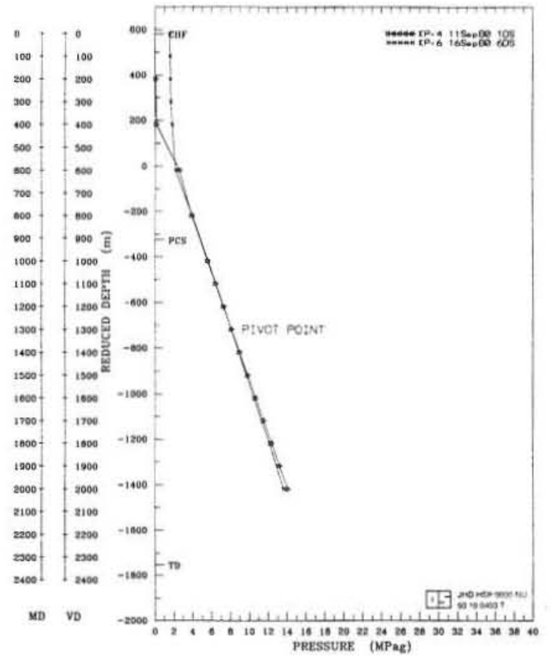

FIGURE 3: Well MG-1 pressure control point

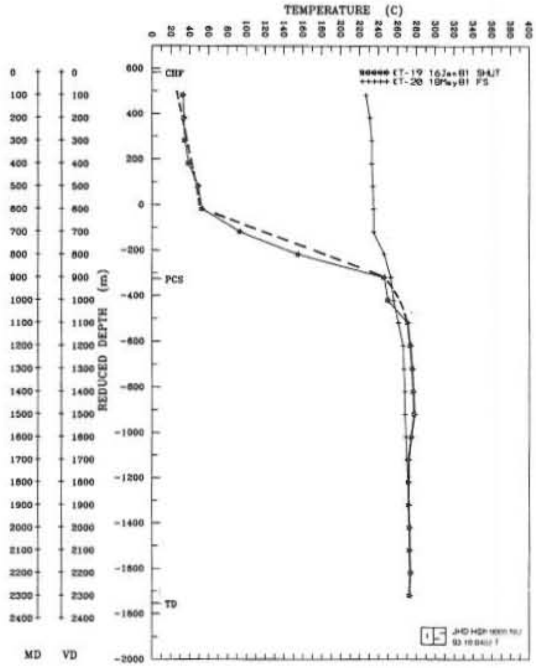

FIGURE 4: MG-1 stable formation temperature

The stable formation temperature is interpreted to be the one shown in Figure 4. Temperature survey KT-20 shows the temperatures during flowing condition while temperature survey KT-19 shows the temperature at shut-in condition prior to the discharge. The flowing survey fixes the inflow temperature at the bottom to be at 270°C.

Among the 8 wells in the sector this is the only well which can be discharged without being stimulated. Upon discharge the well's massflow was 90 kg/s at a wellhead pressure (WHP) of 1.1 MPa-g. The enthalpy of the fluid was 1358 kJ/kg. The massflow of this well is one of the highest and is indicative of the good permeability in the vicinity.

2.1.2 Well MG-2D

MG-2D was drilled to test the southeastern flank of the sector. Completion tests quantified the injectivity index of the well to be 66 l/s-MPa and its transmissivity as 6.0 Dm. Upon consideration of the heat-up and flowing surveys the permeable zones are interpreted as follows: around -532, -882, -1008 and -1272 m a.m.s.l.. The pivot point is located at -620 m a.m.s.l. with a pressure of 7 MPa-g as can be seen from Figure 5. Hence, the topmost zone is the major one. The water level in this well is at 200 m a.m.s.l.

Figure 6 shows the stable formation temperature. The flowing temperature survey KT-15 showed that the inflow temperature at the bottom is around 272°C. From the bottom up to about 180 m below the production casing shoe (PCS) the temperatures measured by survey KT-12 are influenced by a downflow hence the formation temperature in this region is greater than those measured by temperature survey KT-12. From the bottom up to the inflow zone at -882 m a.m.s.l.

the rock formation temperature is interpreted to nearly follow the measurements obtained from the flowing temperature survey KT-15. The next reliable point above this inflow zone is the temperature measurement just below the PCS which was not affected by any downflow, hence, the curved line connecting these two points is conceived to represent the formation temperature. In the cased-off portion the formation temperature is taken to be near those obtained by the KT-12 temperature survey.

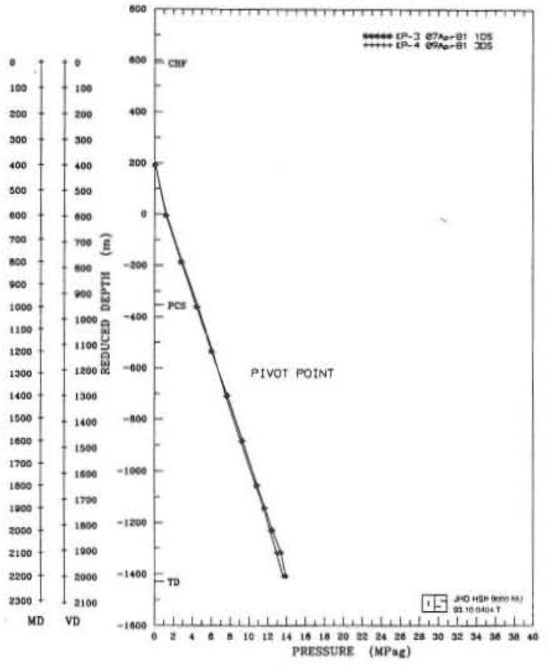

FIGURE 5: Well MG-2D pressure control point

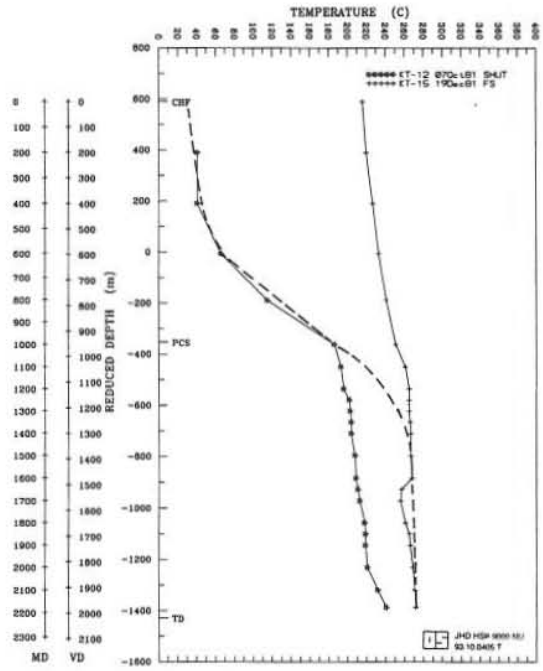

FIGURE 6: Well MG-2D stable formation temperature

The well was stimulated to discharge by injecting steam into it. At a wellhead pressure of 1.1 MPa-g the massflow of the 1140 kJ/kg fluid was 94 kg/s. In comparison with the other wells, this one produces fluids with the lowest enthalpy.

2.1.3 Well MG-3D

MG-3D was drilled to delineate the northeastern boundary of the sector and the completion tests conducted indicated that the well is promising. It has an injectivity index of 68 l/s-MPa and a transmissivity of 12 Dm. These values reflect the good permeability in the area considering that its transmissivity value is the highest. The waterloss test and heat-up surveys indicate that the well has four permeable zones. Just below the PCS is a permeable horizon at -626 m a.m.s.l. The others are located at -743 and -929 m a.m.s.l. and near the bottom. From Figure 7 a pivot point is not evident. However, it is believed that the major zone is the one located at -929 m a.m.s.l. as can be speculated from the flowing temperature survey KT-18 (Figure 8). The water level stabilized at around 250 m a.m.s.l.

In determining the stable formation temperature, the temperatures measured by survey KT-15 from the surface down to the PCS are interpreted to be near it. Just below the PCS down to around -860 m a.m.s.l. the temperatures measured by temperature survey KT-15 are depressed due to the combined effect of colder fluids going down the well and the possibility that the well could still be recovering as temperature survey KT-15 was taken after only a 30 day shut-in period. In determining the stable formation temperature in the region below the PCS the temperatures measured right after the well was in flowing condition (KT-16) and that from the flowing survey (KT-18) were used as a guide (Figure 8). The flowing survey results were lower than the immediate shut-in survey since the highest temperature measured by KT-16 was 300°C while that of KT-18 was only 295°C near the bottom. Considering a reasonable gauge error range of ± 3°C would warrant the assumption that the stable formation temperature near the bottom is about 297°C.

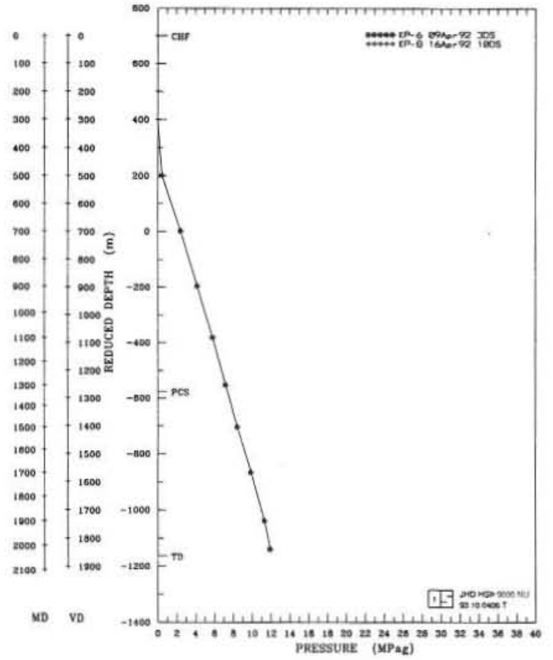

FIGURE 7: Well MG-3D pressure vs. depth graph

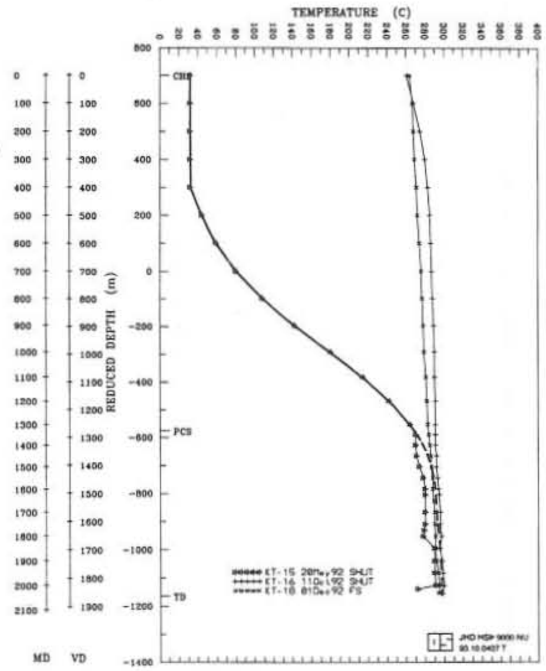

FIGURE 8: Well MG-3D stable formation temperature

The well was stimulated by air compression and the resulting discharge gave a massflow of 72.4 kg/s at a WHP of 0.9 MPa-g. Such a high massflow supports the idea that the northeastern part of the sector has good permeability. The enthalpy of the fluid produced is 2047 kJ/kg, the highest obtained so far. This well also has the highest power potential in the sector at 19 MW_e.

2.1.4 Well MG-4D

Well MG-4D was drilled towards the direction of the Paril Dome in the northern part of the sector and was thought to be above a probable heat source. The completion tests determined the injectivity of this well to be 77 l/s-MPa. Its transmissivity is estimated to be 8 Dm. The permeable horizons for this well are located at around -600 m a.m.s.l. and near the bottom. The pivot point as can be seen from Figure 9 is located at -564 m a.m.s.l. and has a pressure of 7 MPa-g. This implies that the more permeable zone is the upper one. For this well the water level is at 190 m a.m.s.l.

The temperature survey (KT-09) indicates that an isothermal line exists just below the PCS (Figure 10) and that the temperature indicated is lower than those measured above the PCS. Such a profile is due to a massive downflow of colder fluid from the upper permeable zone down to the one at the bottom. This was verified by a spinner survey conducted during the completion tests. With such a copious downflow of fluids it is extremely difficult to determine the stable formation temperature. The only reliable points in this case are the temperature readings at the permeable horizons. The stable formation temperature at the upper permeable zone is taken to be that measured at shut-in condition (KT-09) while at the lower permeable horizon it is measured at flowing condition (KT-20). The stable formation temperature is anywhere between the temperatures measured during shut-in and flowing conditions. Above the upper permeable zone, however, the stable formation temperature is taken to follow that of temperature survey KT-09 as that region is in the cased part of the well.

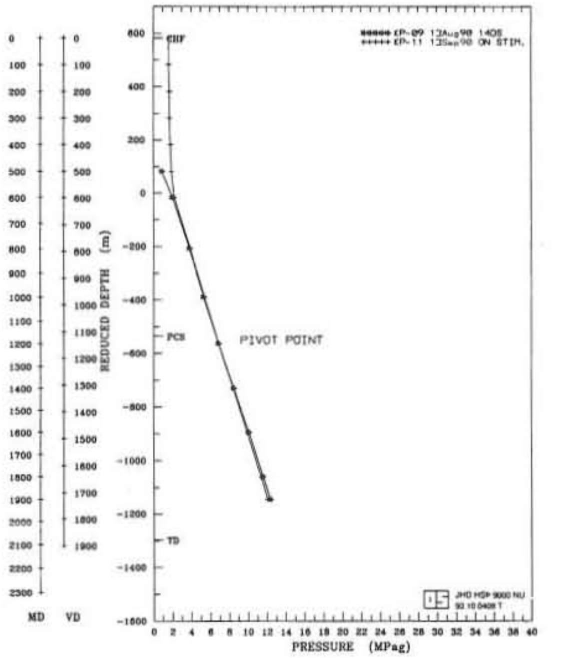

FIGURE 9: Well MG-4D pressure control point

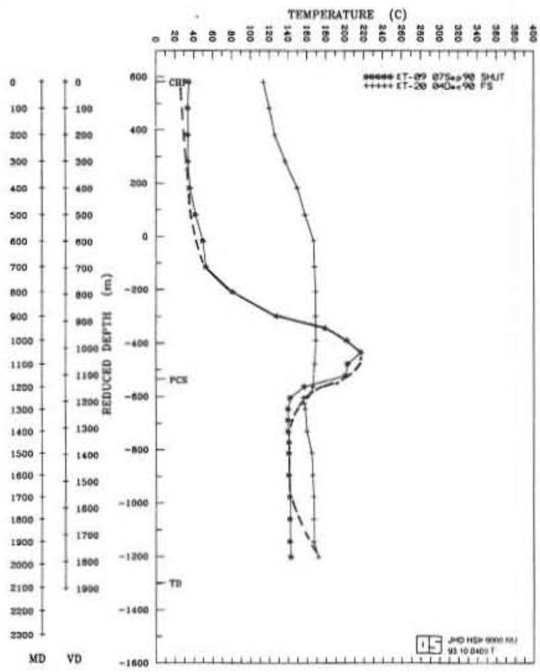

FIGURE 10: Well MG-4D stable formation temperature

The well was stimulated by injecting two-phase fluid from the adjacent well MG-1. The well discharged but the maximum WHP attained was below the commercial WHP of 0.7 MPa-a. The massflow was 20 kg/s and the enthalpy was less than 800 kJ/kg. Such a low enthalpy implies that the upper zone, with a feed temperature of about 140°C, is the one which is dominant during the discharge. The discharge collapsed after 21 days due to the formation of aragonite at the flash point.

2.1.5 Well MG-5D

To test the eastern part of the sector well MG-5D was drilled. The well has an injectivity index of 30 l/s-MPa and a transmissivity of 3.5 Dm. The permeable zones of this well are located at about -531, -620 and -1434 m a.m.s.l. The major permeable zone is thought to be located at -1434 m a.m.s.l. As can be seen from Figure 11 no pivot point is discernable.

The temperature survey KT-09 (Figure 12) indicates a downflow coming from the -620 m a.m.s.l. zone. The temperatures indicated by KT-09 from the upper permeable zones to the bottom are therefore lower than the formation temperature. To set the limits for the formation temperature at the deeper part of the well temperature surveys KT-24 and KT-28 were utilized and the interpreted stable formation temperature is shown in Figure 12.

The discharge tests conducted on the well indicate that the massflow was 30 kg/s at a WHP of 0.8 MPa-g. The enthalpy of the fluid was 1350 kJ/kg. The well has a relatively low massflow and transmissivity values compared to the other wells in the sector indicating that the well is located in an area with less permeability.

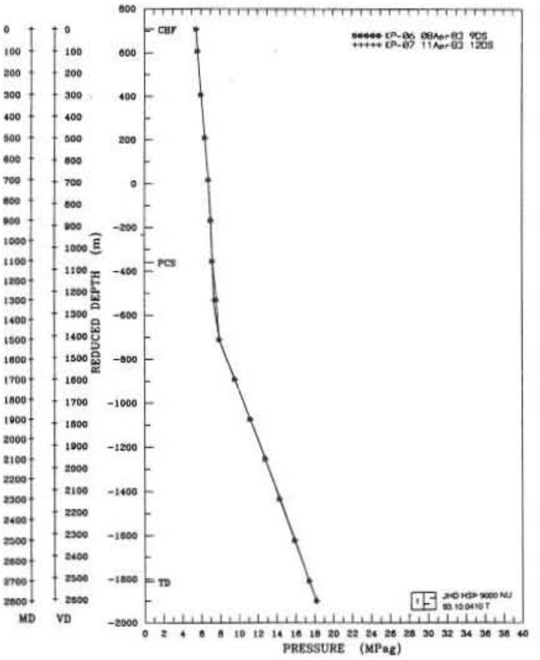

FIGURE 11: Well MG-5D pressure vs. depth graph

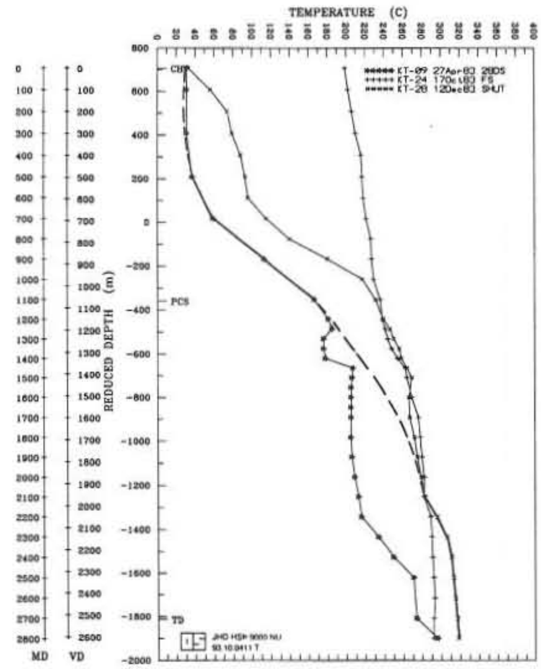

FIGURE 12: Well MG-5D stable formation temperature

2.1.6 Well MG-7D

Well MG-7D was drilled to probe the southwestern extent of the sector. Results of the completion test indicate that the location is a productive area. The injectivity of the well was 157 l/s, the largest measured so far. No pressure fall-off test was conducted due to mechanical difficulties, but as supported by the large injectivity index it could be said that the well has a relatively high transmissivity. The well has at least three permeable zones which are located

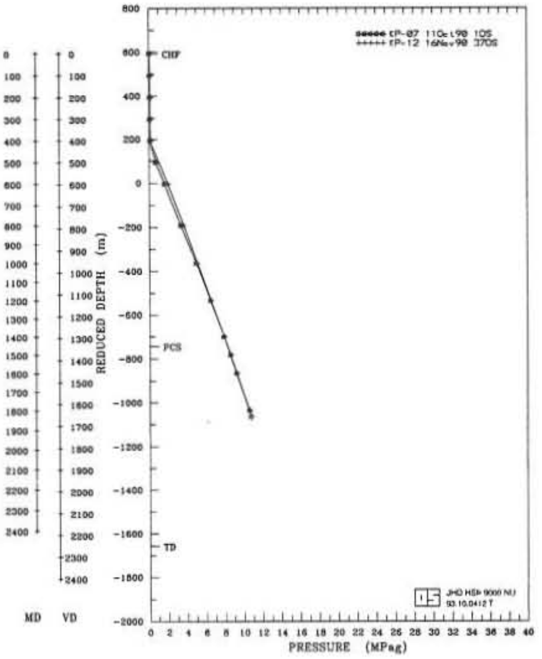

FIGURE 13: Well MG-7D pressure vs. depth graph

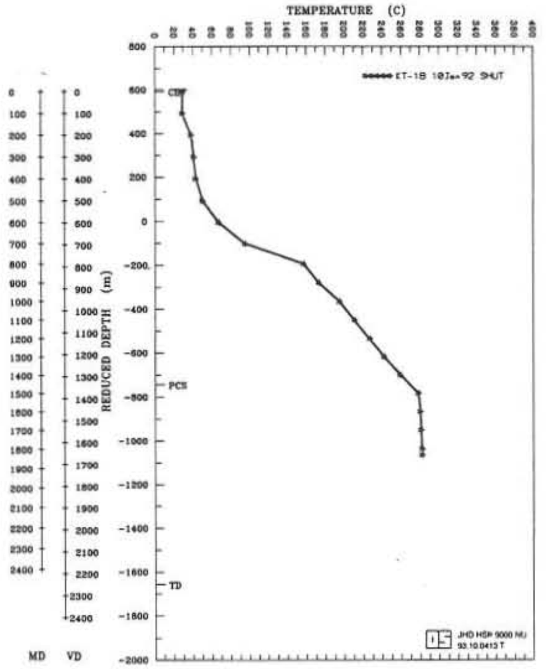

FIGURE 14: Well MG-7D stable formation temperature

at -783, -929 and at -1037 m a.m.s.l. From the available pressure logs (Figure 13) no pivot point is determinable. It's a possibility though that the main production zone is below the bottom of the liner as the liner could not be set at the bottom of the well due to an obstruction caused by a fish left in the hole. The water level is at 200 m a.m.s.l.

The formation temperature is taken to follow the measured temperatures obtained from temperature survey KT-18 (Figure 14). The maximum measured temperature is 281°C at -1036 m a.m.s.l.

The well was discharged and it produced at the rate of 100 kg/s with a WHP of 1.0 MPa-g. The enthalpy of the liquid produced was 1368 kJ/kg. This well has the highest massflow, again indicative of the region's good permeability.

2.1.7 Well MG-8D

The latest well to be drilled in the sector is MG-8D. The injectivity test was conducted with a WHP of 5.2 MPa-g and the resulting injectivity index was 30 l/s-MPa. The transmissivity obtained was low, about 1.4 Dm (Saw, 1993). The high WHP encountered during fluid injection and the low injectivity index and transmissivity value indicate that the well is tight. In fact, no improvement was observed after hydrofracturing was done. The well has two detectable permeable zones at -1377 and -1633 m a.m.s.l. No pivot point could be determined from the pressure profiles (Figure 15). The pressure had not stabilized yet when the last pressure profile was measured since it is still decreasing as the formation releases the pressure acquired during hydrofracturing. This further indicates the tightness or the low permeability of the formations that the well intercepts.

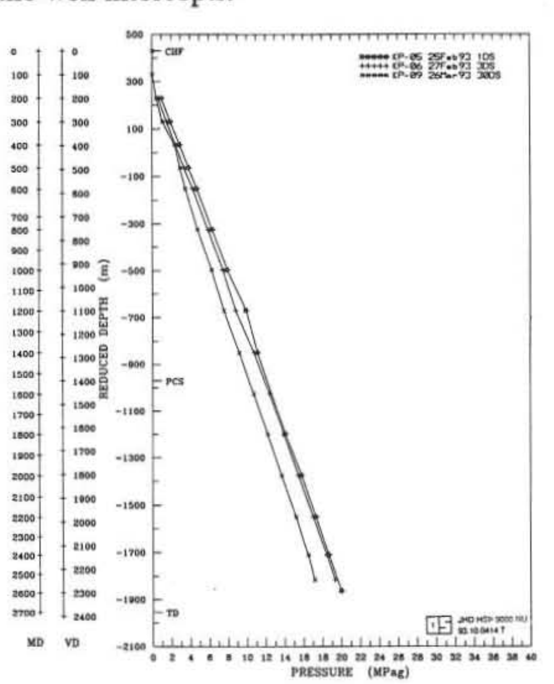

FIGURE 15: Well MG-8D pressure vs. depth graph

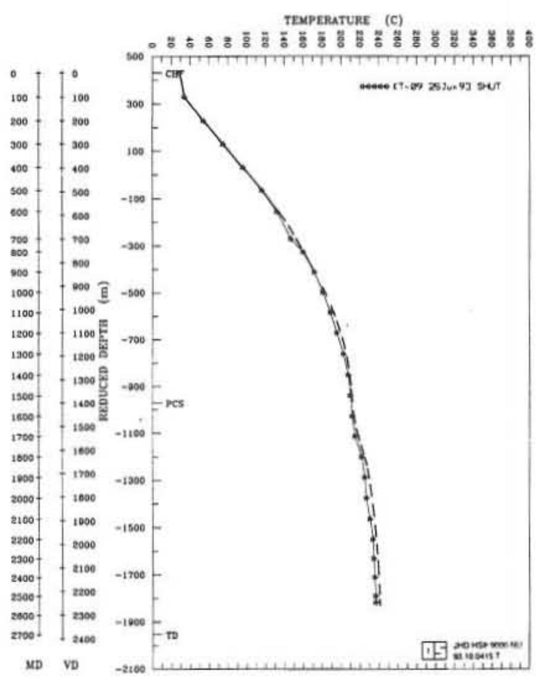

FIGURE 16: Well MG-8D stable formation temperature

The stable formation temperature profile is interpreted to be just a little bit higher than the one measured by temperature survey KT-09 (Figure 16). The maximum measured temperature in this well is about 236°C at the bottom. This well has not yet been discharged.

2.1.8 Well MG-1RD

The first well to be drilled in the Mahanagdong sector which was intended as a reinjection well is MG-1RD. During drilling no loss of circulation fluid was observed and as such the well was expected to be tight. Before the completion tests were conducted hydrofracturing was done in order to improve the well's capacity to accept injection fluids but no improvements were observed. For safety reasons no injectivity test was performed because of the high WHPs (10 MPa-g) which were recorded during injection at the lowest possible flowrates. Also, no pressure fall-off test was done (Urmeneta, 1993). The waterloss survey indicates that there are minor permeable zones around -1317 and -1601 m a.m.s.l. The pressure in the well had not stabilized yet after the hydrofracturing operation when the last pressure profile was measured. No pivot point could be determined from the pressure profiles during the heat-up period (Figure 17). These observations indicate that the overall permeability of the well is quite low.

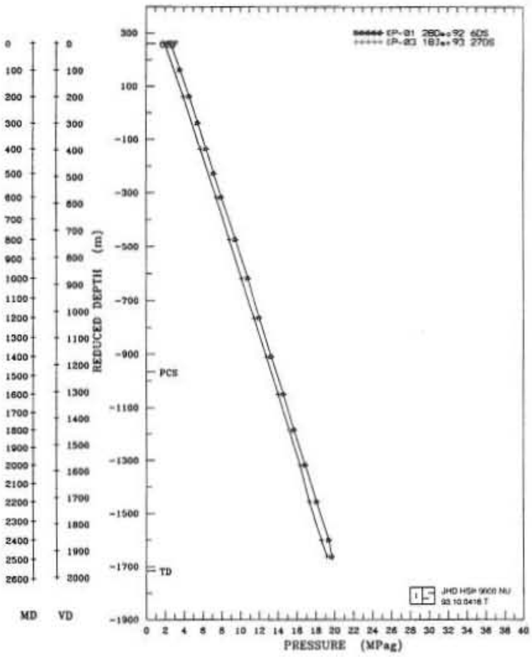

FIGURE 17: Well MG-1RD pressure vs. depth graph

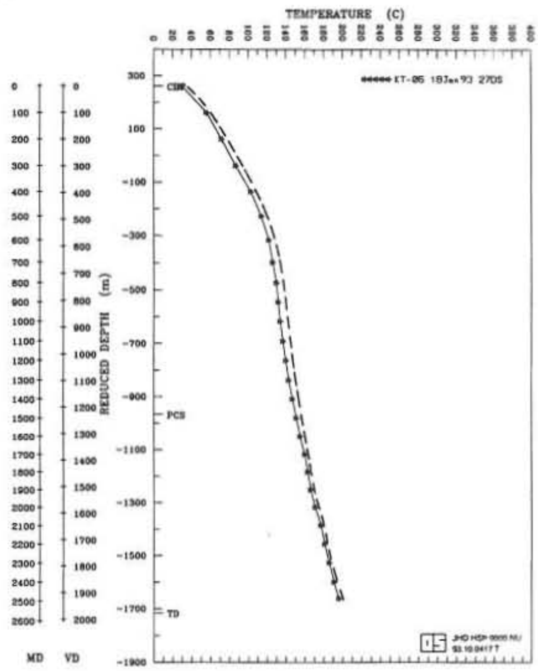

FIGURE 18: Well MG-1RD stable formation temperature

The temperature profile given by temperature survey KT-06 (Figure 18) is interpreted to be near the stable formation temperature. The maximum temperature recorded is 198°C at the bottom of the well. This well has not been discharged yet.

2.2 Fluid chemistry

Of the 8 wells drilled in the area only MG-1RD and MG-8D have not yet been discharged, but the rest of the wells have been tested for its fluid chemistry. Table 1 shows the representative baseline chemistry at throttled discharge conditions. The wells discharge neutral to alkaline waters. Except for MG-4D the reservoir chloride concentrations are almost similar and range from 2500 to 3000 mg/kg. The chloride concentration is highest in the vicinity of MG-3D (Figure 19). The Cl/B ratio is almost similar for all the wells tested except for MG-4D which is affected by the downflow of cold fluids. The silica temperature is highest in the vicinity of MG-3D with the gradient being steeper in the northwestern direction than in the southeastern direction

(Figure 20). In terms of non-condensible gas content by weight MG-5D has the highest values ranging from 1.93% to 4.45%. The data from the wells are notably clustered, indicative of the homogeneity of the thermal fluids in the Mahanagdong reservoir (Bayrante et al., 1992).

TABLE 1: Representative baseline chemistry at throttled discharge conditions (Gonzalez et al., 1993)

Mahanagdong	Cl_{RES} (ppm)	Cl/B	T_{SiO2} (°C)	CO_{2TD} (mm/100mm)	CO_2/H_2S
MG-1	2,700	21.0	267	218	134
MG-2D	2,900	20.7	261	67	80
MG-3D	3,000	---	284	---	---
MG-4D	1,400	27.0	189	---	---
MG-5D	2,500	23.0	266	1,230	306
MG-7D	2,635	21.5	269	202	71

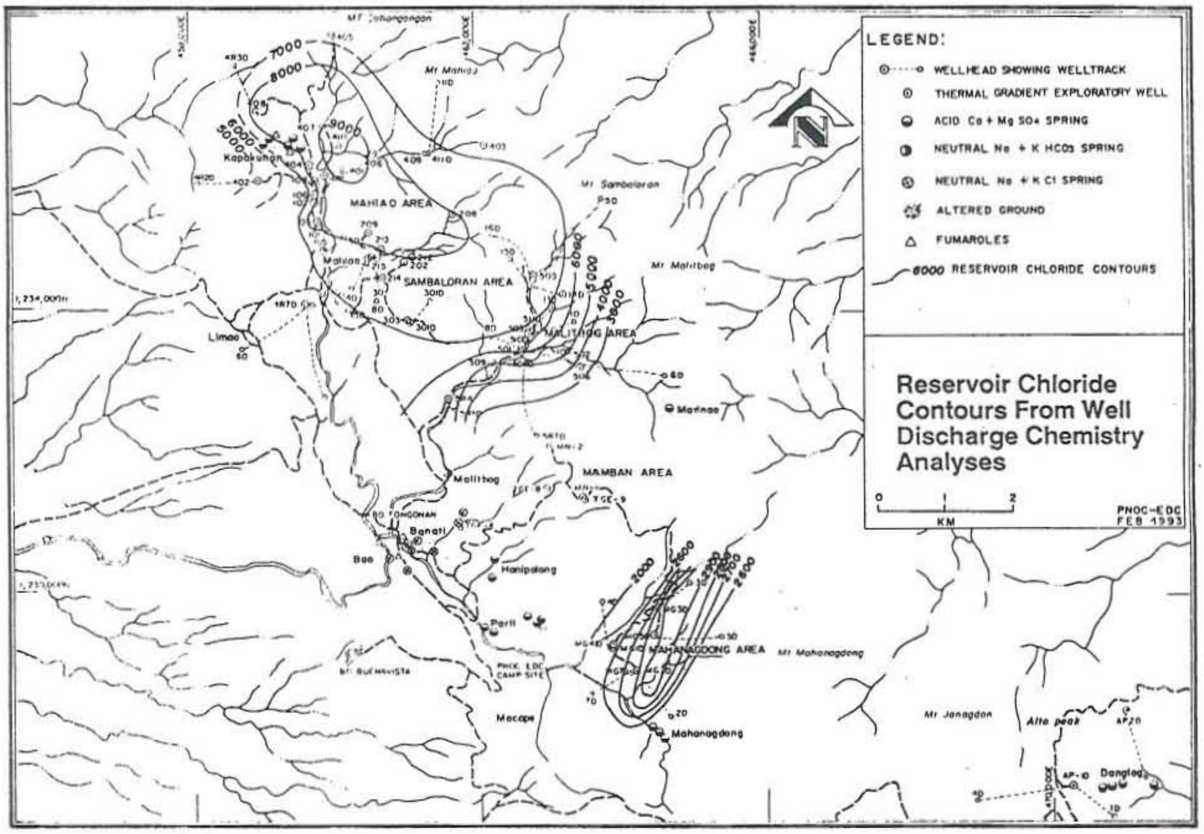

FIGURE 19: Reservoir chloride contours from well discharge chemistry analyses (Gonzalez et al., 1993)

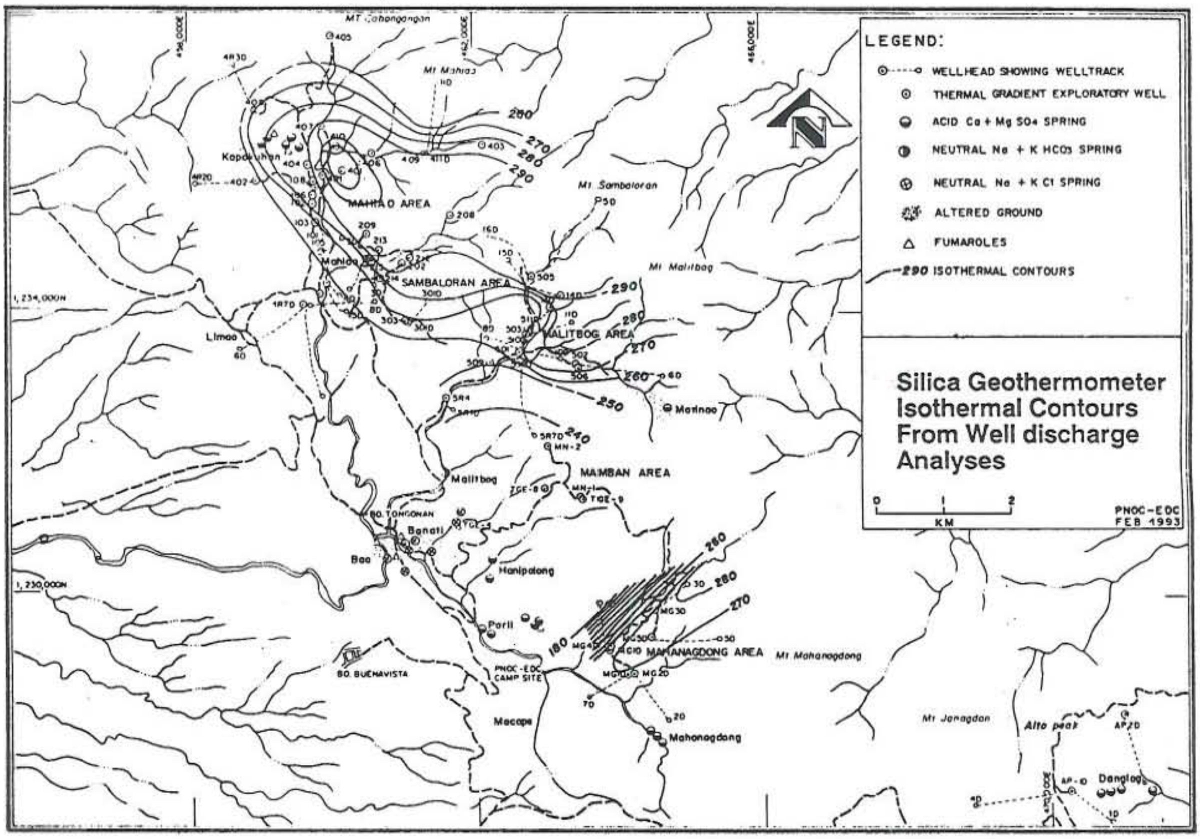

FIGURE 20: Silica geothermometer isothermal contours from well discharge analyses (Gonzalez et al., 1993)

3. RESERVOIR TEMPERATURES AND PRESSURES

3.1 Isothermal maps

The stable rock formation temperatures determined in chapter 2 are the basis for the isothermal maps (Figures 21-23). They are plotted at the elevations: -400, -800, and -1250 m a.m.s.l. The interpolation carried out in between temperature data points have been guided by the location of the pertinent geological structures in the area. From the structural map (Figure 2) it can be seen that MG-4D intersects the Mamban fault. This fault plays an important role as it is expected that this structure copiously conducts cool and dilute fluids which detrimentally affect MG-4D. Along this fault the temperature contours tend to bunch up as it acts like a barrier. Towards the southwest two structures channel hot reservoir fluids and they are the central fault line and the Mahanagdong fault. These would serve as highways for the hot fluid as it flows towards the southeastern part of the Mahanagdong sector. Further to the west is the west fault line and is interpreted as a barrier. The presence of these structures was taken into account when the contours were drawn. The general shape of the contours is consistent with the silica geothermometer isothermal contours (Figure 20).

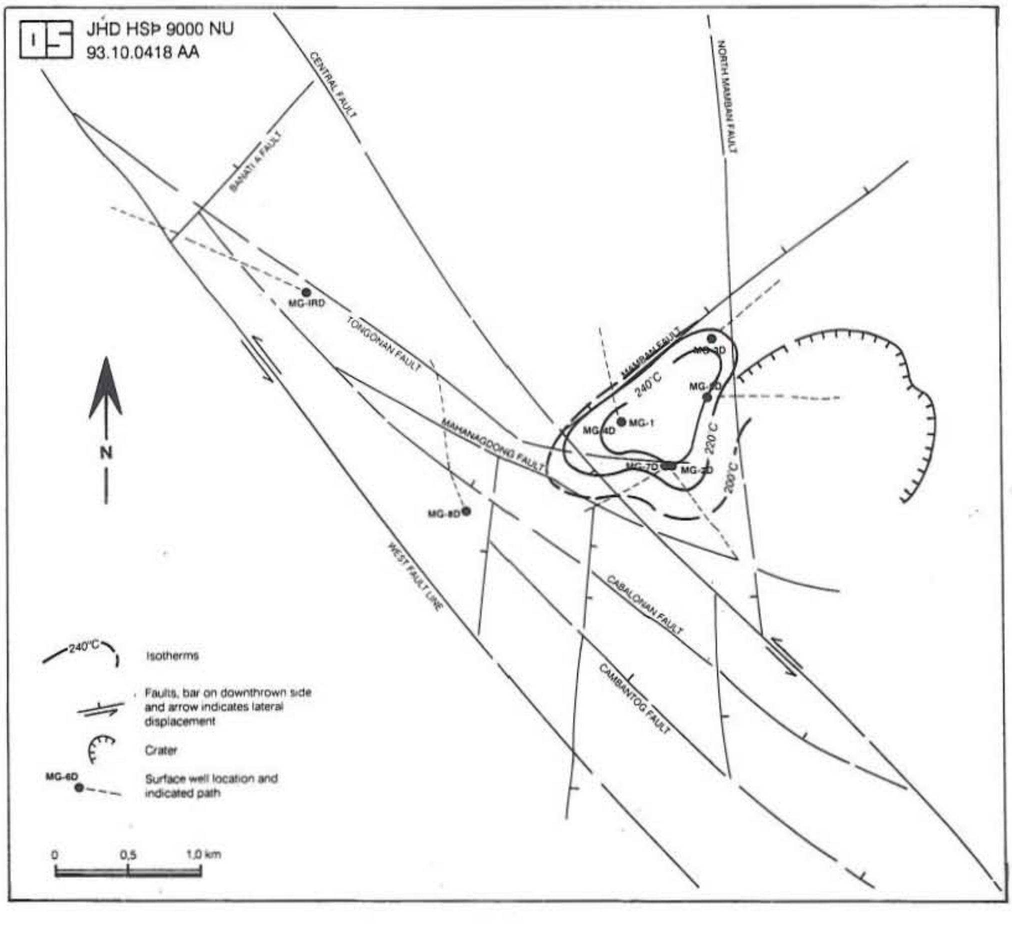

FIGURE 21: Isothermal contours at -400 m a.m.s.l. from downhole measurements

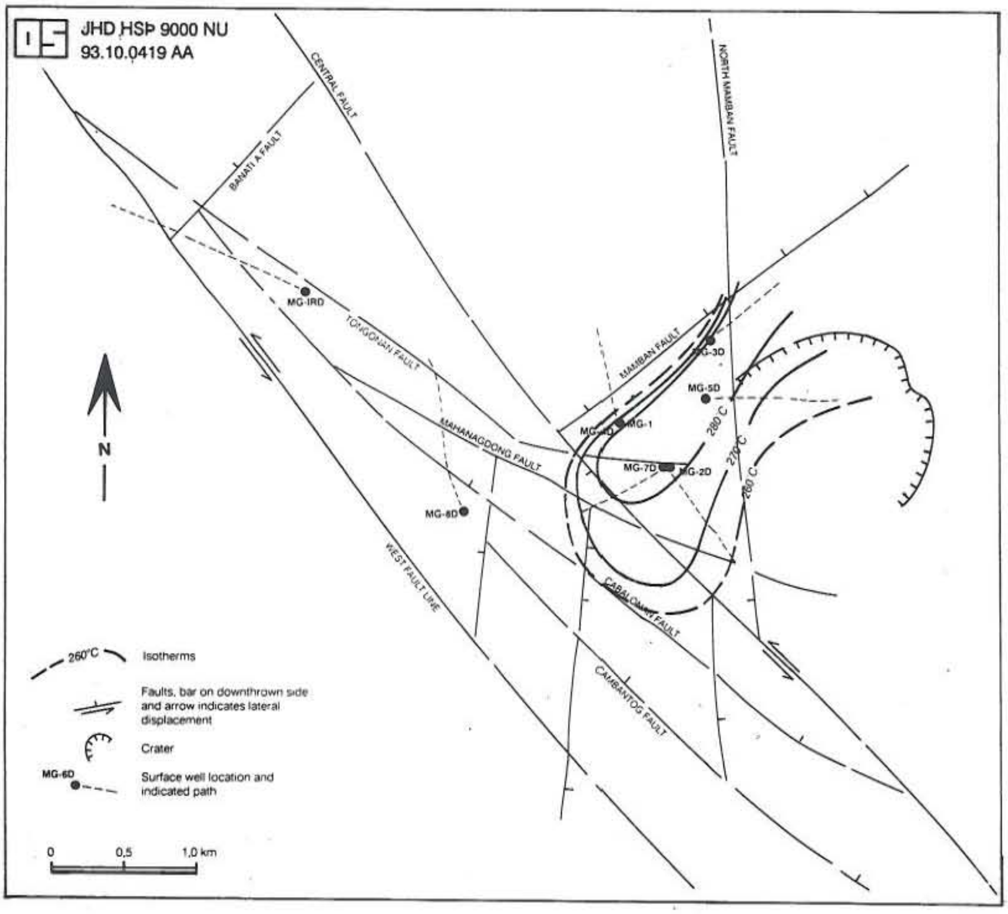

FIGURE 22: Isothermal contours at -800 m a.m.s.l. from downhole measurements

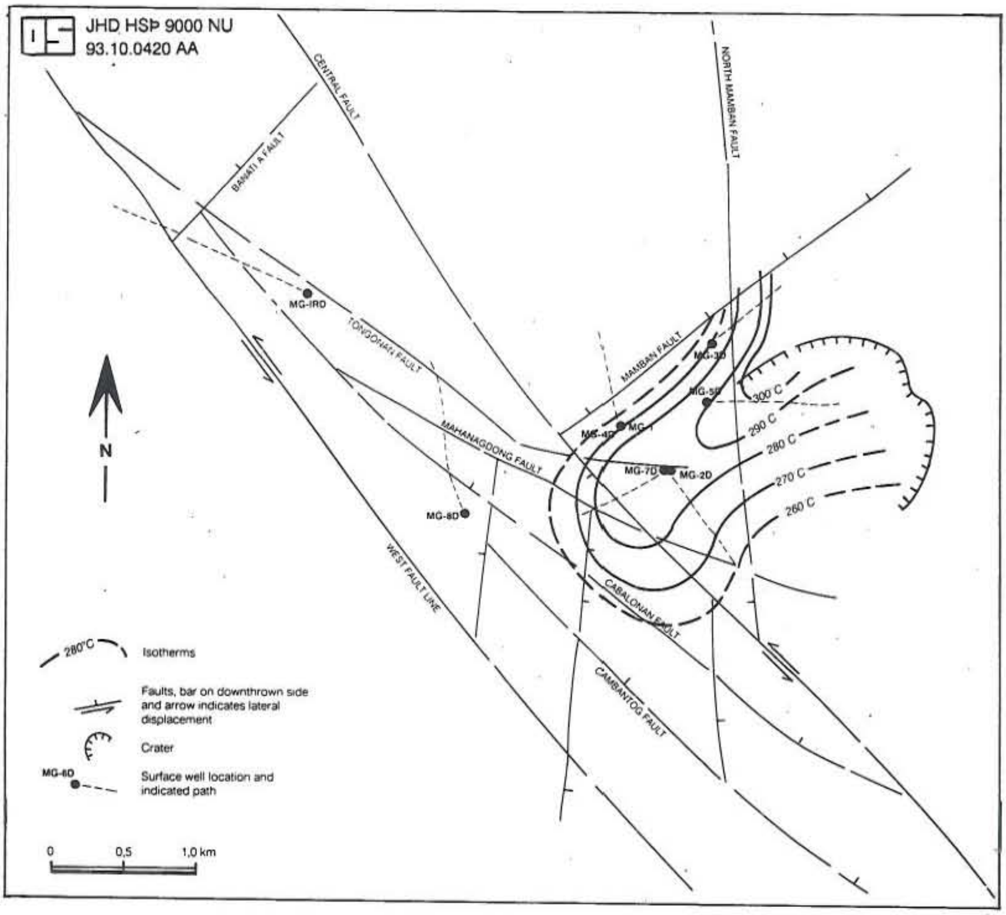

FIGURE 23: Isothermal contours at -1250 m a.m.s.l. from downhole measurements

3.2 Isobaric map

Pressure values from the determined pivot points were used and extrapolated to a reference depth of -1250 m a.m.s.l. For wells MG-3D, MG-5D, MG-7D, MG-8D and MG-1RD where no pivot points were observed, the measured pressure values at -1250 m a.m.s.l. where utilized keeping in mind that the true reservoir pressure could either be lower or higher than these values. The pressure map (Figure 24) shows an increasing pressure gradient towards the northeast. The highest pressures are located in the MG-3D and MG-5D area (13 MPa-g), but are decreasing toward the southern part of the Mahanagdong sector. In well MG-4D the pressure is anomalously high which could be explained as an effect of the cold downflowing liquid in that well.

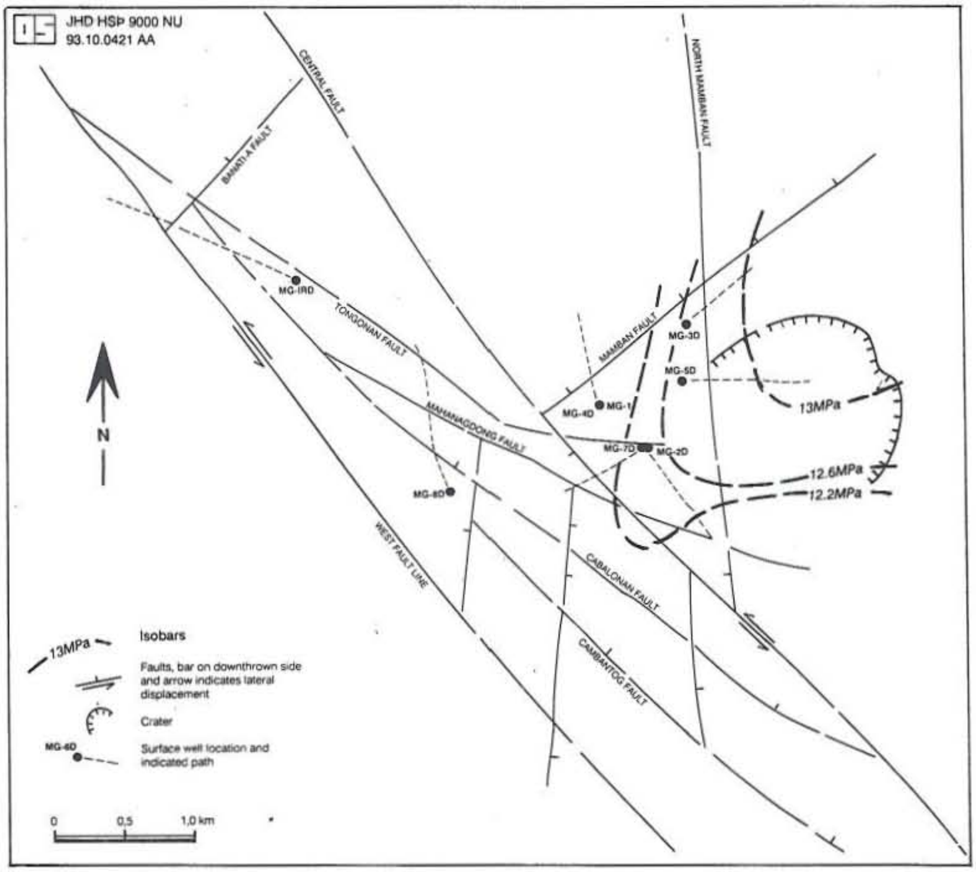

FIGURE 24: Isobaric contours at -1250 m a.m.s.l. from downhole measurements

4. CONCEPTUAL RESERVOIR MODEL

Several conceptual models for the natural state of the GTGF have been presented. Whittome and Smith (1979) proposed a model for the GTGF and posed the question whether the field has one or two heat sources. This came about as a consequence of the fact that some aspects of the geochemistry are not compatible with a single source reservoir model. It has been speculated that in order to explain the observed geochemical parameters the GTGF is composed of two systems overlapping near the Bao Valley. In the succeeding studies conducted the existence of a geothermal system in the Mahanagdong-Paril area which is hydrologically unconnected to the Mahiao-Sambaloran-Malitbog system has been established (PNOC-EDC, 1990). The conceptual model identifies the upflow zone in the Mahiao-Sambaloran-Malitbog system to be in the area enclosed by wells 407, 409, 208A, 215, 105, 108 and 404 (Figure 25) and the outflow region to be the Bao Valley (Gonzalez et al., 1993). In the Mahanagdong sector of the GTGF, the upflow zone, based on the available data at that time, is diffused. The most likely upflow zones are speculated to be near the vicinity of wells MG-1 and MG-7D and presumably at the Paril dome. The outflow of this system was expected to be to the Bao Valley (Gonzalez et al., 1993).

The working conceptual reservoir model for the Mahanagdong system used in this study is quite different. The isothermal and isobaric maps (Figures 23 and 24) suggest that the upflow zone is located in the northeastern part of the sector (near well MG-3D) with the temperature in that area being greater than 300°C. This temperature is the highest temperature measured at around -1140 m a.m.s.l. in well MG-3D. The well was completed prematurely due to collapsing formation but had it been drilled according to plan then it could have encountered fluids with temperature greater than 300°C. The location of this hot area is also reflected in the silica geothermometer isothermal contours (Figure 20). Aside from this the highest reservoir chloride concentration is within this region (Figure 19). From a study conducted by Sanchez (1993) on the Mt. Labo geothermal prospect, the high Cl^- concentrations in the wells have been accounted to be primarily due to magmatic degassing since andesitic rock dissolution would normally account for just 200

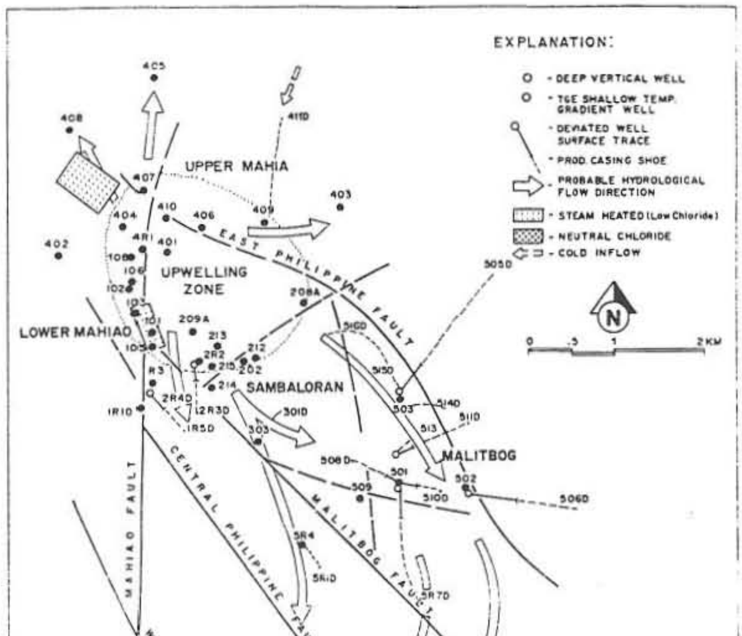

FIGURE 25: Probable hydrological flow directions in the GTGF (Gonzalez et al., 1993)

ppm. This implies that in areas where the Cl^- concentration is high and can not be accounted for by rock dissolution alone, the higher the Cl^- concentration is in an area the nearer it is to the heat source. This seems to be the case for the adjoining Mahiao-Sambaloran-Malitbog system wherein the highest reservoir chloride concentration is located in the upflow region (Figure 19). From the conceived upflow zone the fluid then moves towards the southwest along the direction of the Mamban fault. The Mamban fault which copiously conducts cold fluids is treated as a barrier thus preventing the flow towards the northwest. The treatment of the Mamban fault as a barrier is warranted on the fact that the temperature in the area around well MG-1 has not been severely affected by these cold fluids. Well MG-1 is nearest MG-4D and lies on the side of the fault towards the southeast. As the fluid goes towards the southwest direction it intersects the North Mamban fault. This fault, which is the major structure separating wells MG-3D and MG-5D from the rest, is treated as a flow retardant as suggested by the results of the interference test. Well MG-3D was discharged and the observation wells chosen for the test were MG-1 and MG-7D. The results showed no clear pressure interaction between the wells (Gonzalez et al., 1993). In fact, there is about 1 MPa pressure difference between the areas lying on opposite sides of the North Mamban fault as exemplified by the pressures at wells MG-1 and MG-5D at -1250 m a.m.s.l. (Figure 24). As the hot fluid reaches the central fault, a known conduit for hot geothermal fluids, it is diverted to the southeast. The drilling of wells MG-1RD and MG-8D led to the idea that the outflow of the Mahanagdong system could not be towards the Bao Valley in the northwest as the wells proved to be very tight. As a matter of fact, the consultant team Mesquite Group, Inc. et al. (1993) discounted the interpretation of the Bao-Banati springs being an outflow of the Mahanagdong sector. Therefore, the main difference between this conceptual model and the previous model is the location of the heat source and the outflow.

5. RESERVOIR MODELLING AND NATURAL STATE SIMULATION

5.1 Simulation code and methodology

To simulate the coupled transport of water, vapour, air and heat in a porous medium the simulation code TOUGH was used. It is a member of the MULKOM family of multi-phase, multi-component codes, which was developed at the Lawrence Berkeley Laboratory primarily for geothermal reservoir applications (Pruess, 1983). The TOUGH simulator treats the flow of both liquid and gas due to pressure, viscous and gravity forces according to Darcy's law with the interference between the phases represented by relative permeability functions. Heat transport occurs through conduction, convection and binary diffusion. It also provides an option to specify the withdrawal or injection of either heat or mass.

The process of simulating a geothermal reservoir in its natural state starts with the formulation of a conceptual model. The conceptual model is then translated into a numerical model by considering a grid system and in this case a three dimensional numerical grid was utilized. Physical properties such as permeability, porosity, rock density, thermal conductivity, heat capacity and the like, together with the initial and boundary conditions are specified to run the numerical model. The Mahanagdong sector of the GTGF is a dynamic system in its natural state. Changes

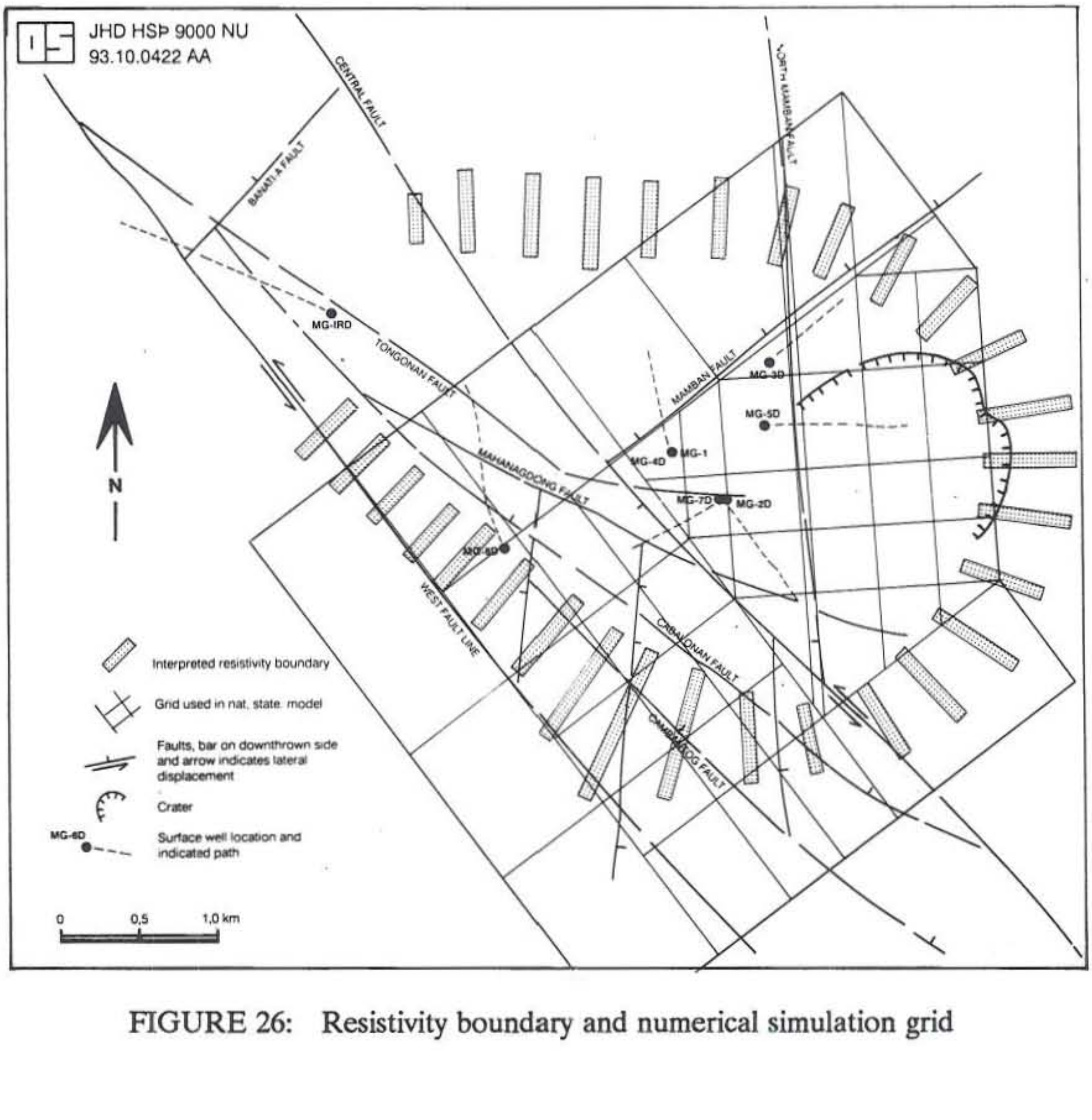

FIGURE 26: Resistivity boundary and numerical simulation grid

happening in the system are thought to be small and are perceived to be near dynamic equilibrium and being so, the model has to be run until a steady-state approximation is achieved. The permeabilities and other physical parameters are adjusted through a series of trial and error runs until a good match with the observed pressures and temperatures is obtained. A best model has thus been produced.

5.2 Reservoir model description

The areal extent of the simulation grid has been based primarily on the area covered by the interpreted resistivity anomaly zone (Figure 26). It covers an area of 17.3 km^2 and its asymmetric shape is based on the geological structures which play an important role in the hydrothermal flow. The grid was made in such a way that no two wells occupy the same block. For the reservoir layers there are 56 blocks in each one.

The vertical extent of the model is from +400 to -2000 m a.m.s.l., equivalent to a thickness of 2.4 km. It has 6 layers which have been labelled as layers G, I, A, B, C and D (Figure 27). The centre of each layer is located at +200, -100, -400, -800, -1250 and -1750 m a.m.s.l., respectively. The reservoir has been taken to start at layer A where the average temperature is about 220°C. This criterion for setting the location of the top of the reservoir is the same one used in the volumetric stored heat calculations (Gonzalez et al., 1993). The rest of the reservoir region has been subdivided in such a way as not to have layers which are more than 500 m thick. Above layer A is a 200 m layer I which has been designated as the caprock due to the fact that the temperature profile indicates that this region primarily transfers heat through conduction. Above layer I is the 400 m layer representing the groundwater system. The model has a total number of 257 elements.

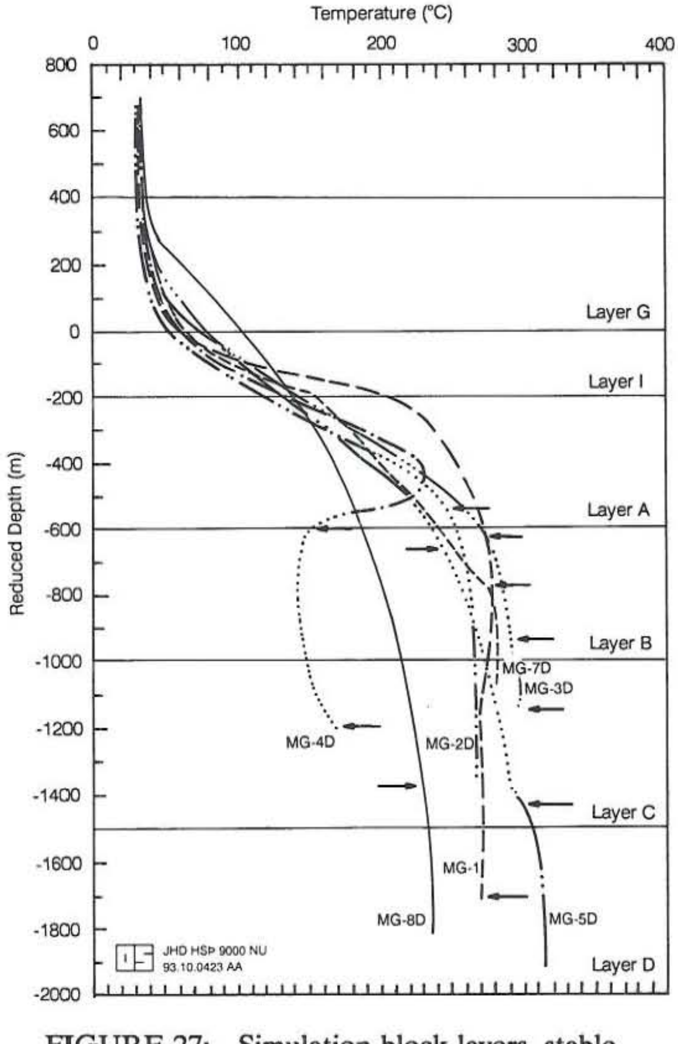

FIGURE 27: Simulation block layers, stable formation temperatures and feed zones

For the reservoir layers the general horizontal permeability distribution in each layer is generally characterized by the permeability distribution in layer C as shown in Figure 28. The upflow region is likewise specified in the figure. At the bottom of this upflow region is a source element of the same shape with a thickness of 1 m. It is through this element that mass is injected in order to simulate natural recharge into the system. The North Mamban fault which acts as a flow retardant is represented by the 0.50 mD blocks. The area where the geothermal fluid is thought

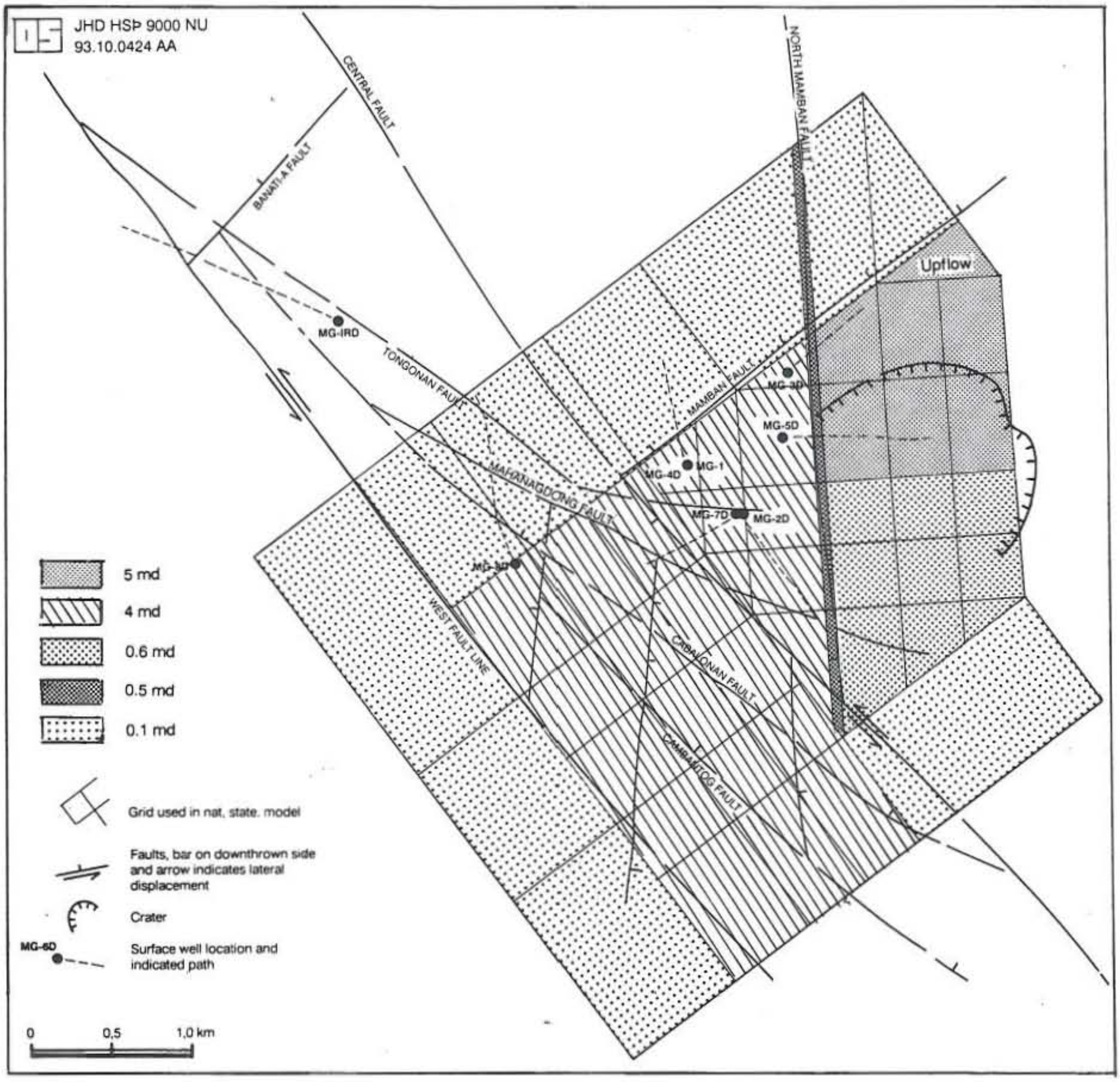

FIGURE 28: Permeability distribution in layer C

to pass through is given a permeability value of 4 mD. The outer blocks are the boundary blocks and were given a relatively low permeability value of 0.1 mD. The permeability distribution in the vertical direction ranges from 0.01 to 8 mD while in the horizontal direction it's between 0.01 to 5 mD. The part of the Mamban fault which is interpreted as a barrier separates wells MG-4D and MG-1 (Figure 26). The interface area between these blocks were designated values which are one-third of their actual areas in order to simulate a barrier. A constant temperature and pressure condition is imposed on the boundary at the reservoir layers and this is achieved by connecting the periphery blocks to very large (in the order of $1x10^{11}$ km^3) volume elements with very high permeability (100 mD). These elements serve to accept any fluids coming out of the geothermal system.

In the caprock, layer I, the number of blocks were reduced from 56 to 12. In layer G the number of blocks were further reduced to 4. These are the upper layers where details are not so important since they are above the reservoir. Layer G in particular just represents the groundwater system.

A total of 6 rock types were utilized. A porosity value of 6% and a rock density of 2600 kg/m^3 was used in the model based on the measurements obtained by Bayrante (1991). In the fault and the volume blocks, however, a 10% porosity was used. The model assumes a rock specific heat of 900 J/kg°C which is the same value used in the volumetric stored heat calculations of Gonzalez et al. (1993). Salera and O'Sullivan (1987) used the same value also for their model of the Mahiao-Sambaloran-Malitbog sector of the GTGF. Table 2 shows a summary of the rock properties used.

TABLE 2: Rock properties used in the numerical model

Rock type	Density (kg/m^3)	Porosity (%)	Permeability (mD) k_1	k_2	k_3	Thermal conductivity (W/m°C)	Heat capacity (J/kg°C)
fault	2600	10	2.00	0.50	2.00	1.90	900
capro	2600	6	0.01	0.01	0.01	1.10	900
upflo	2600	6	5.00	0.60	8.00	1.90	900
reser	2600	6	4.00	2.00	3.00	1.90	900
bound	2600	6	1.50	0.10	1.00	1.90	900
volum	2600	10	100.00	100.00	100.00	1.90	900

A heat flux of 0.17 W/m^2 was added at the bottom through all the elements except at the upflow zone where a 1373 kJ/kg (305°C) fluid is being injected at the rate of 20 kg/s. Heat sinks were also placed at the top elements to represent the conductive heat losses to the environment. These sinks maintain the ground temperature at a constant level.

It was also assumed that the relative permeabilities depend linearly on the saturation. The immobile water and steam saturations were 0.30 and 0.05, respectively. The water and steam become completely mobile when the saturation levels reach 1 and 0.7, respectively.

The simulation runs were started with the blocks being "cold". The initial pressures and temperatures were taken to be near those exhibited by MG-1RD, a well very far from the reservoir. By doing this, one sees the evolution of the system into its current state.

5.3 Natural state simulation results

A near steady state condition was achieved after the numerical model was run for 10,000 years. The results indicate that the model was able to duplicate the general direction of the fluid flow as suggested by the simulated isothermal and isobaric contours at -1250 m a.m.s.l. (Figures 29 and 30).

Comparing the simulated and measured temperatures in well MG-1 (Figure 31) it can be said that the simulated temperatures duplicate the measured ones. The same can be said about well MG-3D (Figure 31). In well MG-4D we can see that the model was able to simulate the temperature reversal (Figure 31). In wells MG-2D, (Figure 31) and MG-5D and MG-7D (Figure 32) the simulated temperatures are near the measured ones. It is only in well MG-8D where the calculated temperatures are all below the measured ones (Figure 32). This is not a serious problem since the well is situated in the boundary. However, this will just place the model on the conservative side.

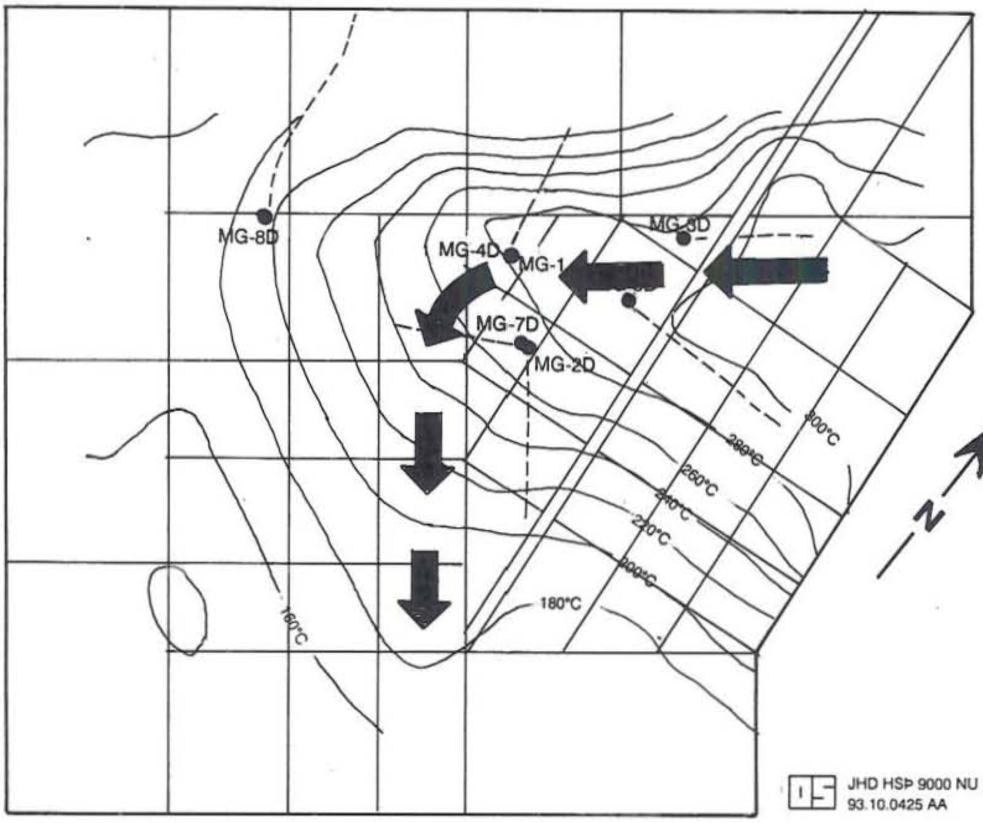

FIGURE 29: Simulated isothermal contours at -1250 m a.m.s.l.

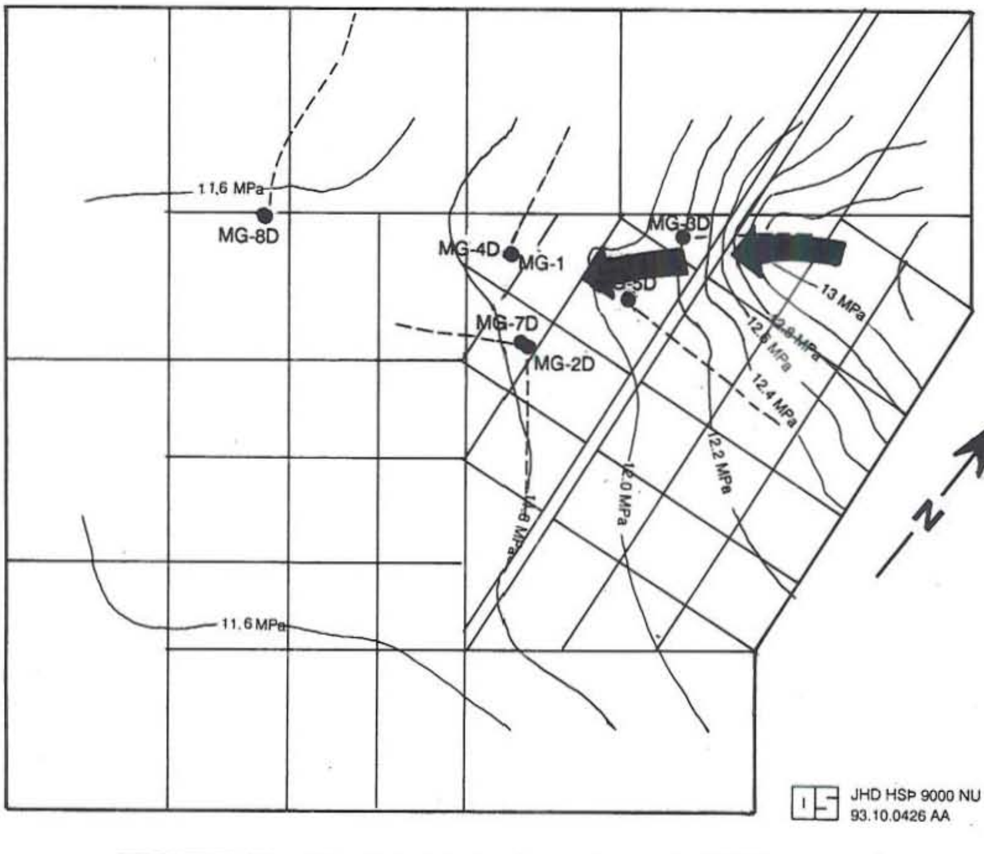

FIGURE 30: Simulated isobaric contours at -1250 m a.m.s.l.

The pressures have been matched to within an error range of ±1 MPa in all the wells except MG-4D and MG-8D (Figures 33 and 34). In case of well MG-4D the underpressurization at the lower part of the well is just apparent since the measured values at these depths are high due to high measured pressures being maintained by the cold downflow in the well. In the case of well MG-8D the underpressurization is apparent as the measured pressure is expected to be high because it had not stabilized yet after the hydrofracturing operation, when it was measured.

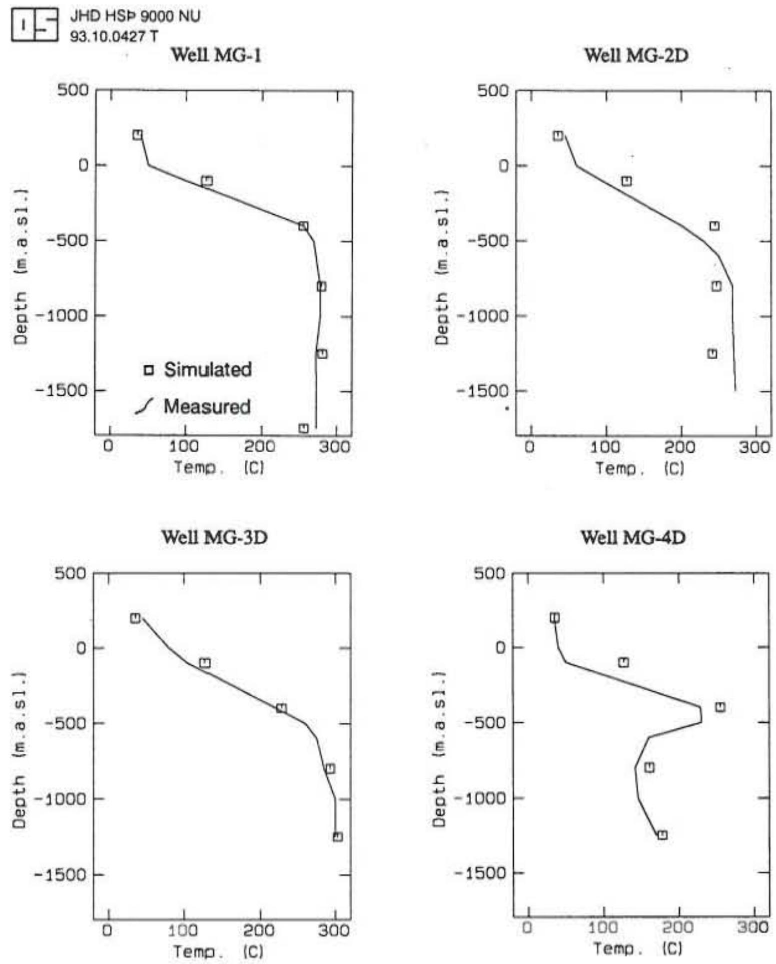

FIGURE 31: Measured and simulated temperatures in wells MG-1, MG-2D, MG-3D and MG-4D

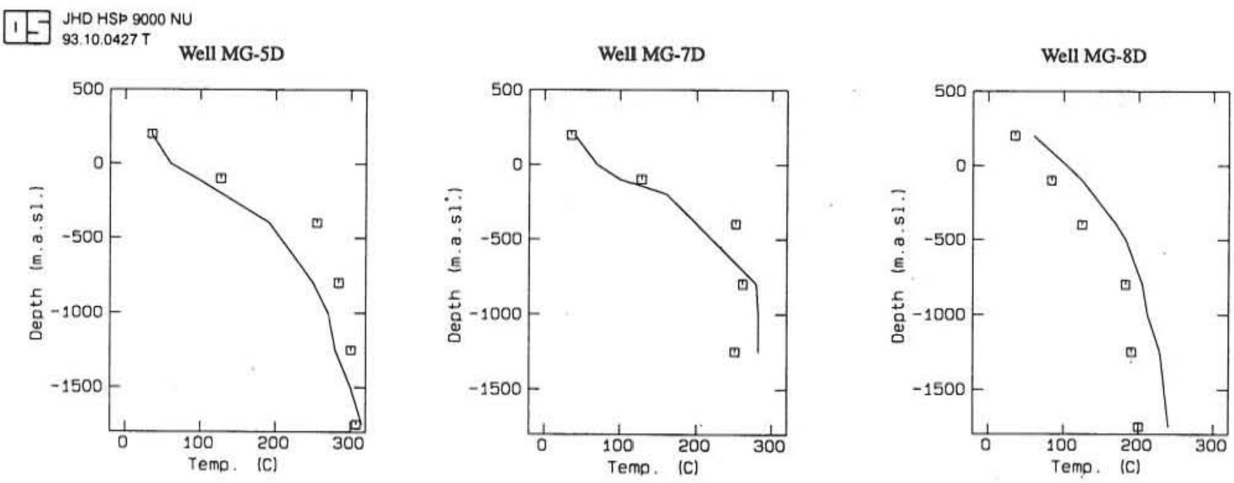

FIGURE 32: Measured and simulated temperatures in wells MG-5D, MG-7D and MG-8D

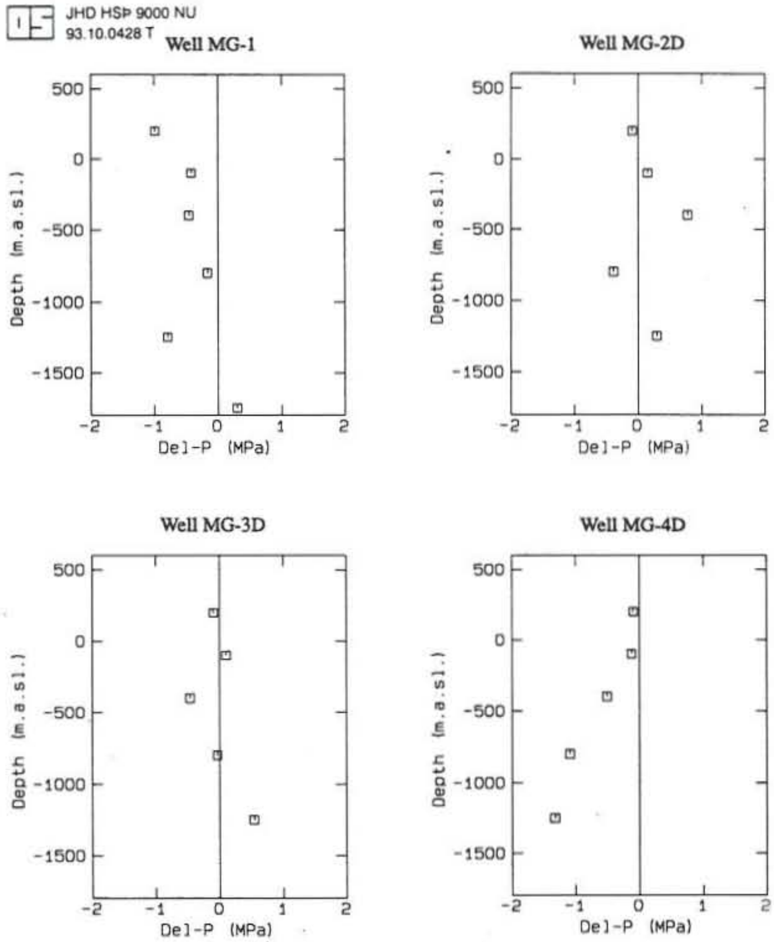

FIGURE 33: Difference between measured and simulated pressures in wells MG-1, MG-2D, MG-3D and MG-4D

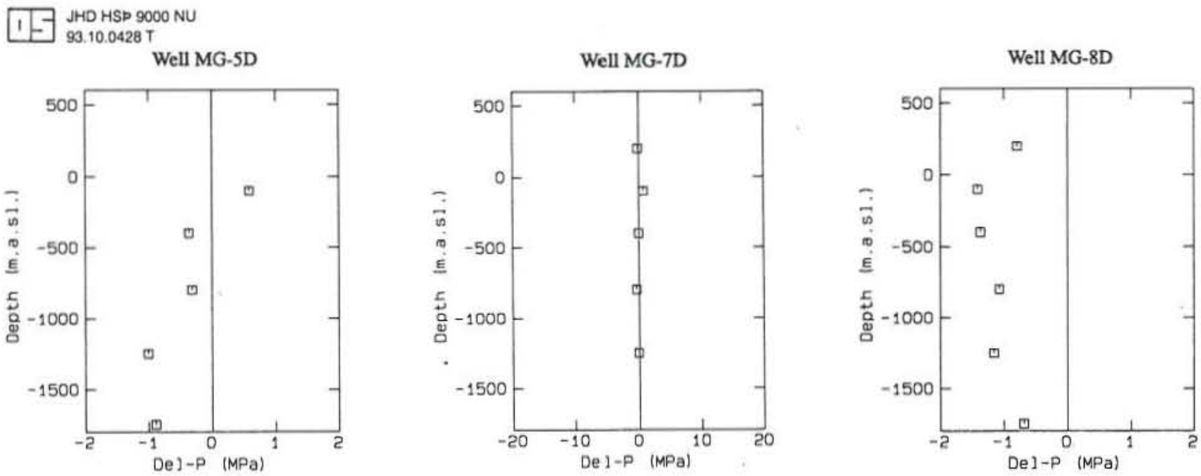

FIGURE 34: Difference between measured and simulated pressures in wells MG-5D, MG-7D and MG-8D

6. CONCLUSIONS AND RECOMMENDATIONS

The numerical model for the Mahanagdong sector of the Greater Tongonan geothermal field in its natural state was successful in duplicating the probable hydrothermal flow in the system. On the per well basis, it was able to reasonably simulate the measured temperatures and pressures. As such, the permeability distribution of the system has been determined based on the assumed recharge rate. Preliminary simulation runs for the exploitation of the sector have been made with the current model. The runs indicate that up to around 17 wells may be needed initially to satisfy the proposed 165 MW_e plant capacity. The model indicates that the sector can sustain that capacity until the tenth year without reinjection. By that time about 18 make-up wells should have been drilled. After that period the current model for the sector indicates that it can not support the loading of 165 MW_e and the generating capacity will decline. For pressure support reinjection could be done in order to push further the productive lifespan of the sector. However, the storage parameters have not yet been calibrated against an ample set of production data and the number of wells needed initially and during the lifespan of the power plant could change depending on the calibration. In the event that such data is made available it is recommended that fine tuning of the model in terms of the storage parameters and the permeability distribution corresponding to the specified recharge rate should be made in order to simulate the production history of the field. It is further recommended that the volume of the elements near wells should be made smaller in order to duplicate the measured enthalpies. These refinements are necessary in order to give reasonable predictions as to the behaviour of the system under exploitation.

ACKNOWLEDGEMENTS

The author wishes to thank Dr. Ingvar B. Fridleifsson and Ludvik S. Georgsson for providing him the opportunity to attend the UNU Geothermal Training Programme and for the guidance and assistance extended to come up with this report.

It would have been impossible to come up with the figures if not for the help of Audur Agustsdottir and Sylvia Johannsdottir. Proofreading was done by Margret Westlund and to these ladies, thank you.

Gratitude is expressed to the reservoir engineering group of Orkustofnun especially to

- Benedikt Steingrimsson for helping out on well data interpretation,
- Dr. Thordur Arason and Grimur Bjornsson for making data processing and interpretation a lot easier,
- and to Dr. Valgardur Stefansson for his invaluable comments.

To the person who supervised this study, Omar Sigurdsson: thank you for providing the right atmosphere for learning, the interesting and intellectually stimulating discussions and for meticulously reviewing the text.

REFERENCES

Aunzo, Z.P., Sarmiento, Z.F. and Sarit, A.D., 1986: The simulation of the Tongonan geothermal field. The initial state: Preliminary result. Proceedings of the 8th New Zealand Geothermal Workshop, University of Auckland, 135-140.

Bayrante, L.F., 1991: Porosity and density measurements of Mahanagdong core samples. PNOC-EDC, internal report, 7 pp.

Bayrante, L.F., Rodis, N.O., Reyes, A.G., and Sanchez, D.R., 1992: Resource assessment of the Mahanagdong geothermal project, Leyte, Central Philippines. Proceedings of the 14th New Zealand Geothermal Workshop, University of Auckland, 171-178.

Gonzalez, R.C., Ogena, M.S., Salera, J.R.M., Bayrante, L.F., Vergara, M.C., Malate, R.C.M., Solaña, R.R., Sanchez, D.R., and Clemente, V.C., 1993: Integrated resource assessment, Greater Tongonan geothermal field. PNOC-EDC, internal report, 231 pp.

Mesquite Group Inc. and Harding Lawson Associates Dames and Moore, 1993: Resource assessment review update: Mahanagdong sector, Greater Tongonan geothermal field. A memorandum report prepared for the PNOC-EDC Geothermal Division, 31 pp.

PNOC-EDC, 1990: Preliminary resource assessment, Mahanagdong sector, Greater Tongonan geothermal field. PNOC-EDC, internal report, 47 pp.

PNOC-EDC, 1991: Resource assessment update, Mahanagdong sector, Greater Tongonan geothermal field. PNOC-EDC, internal report, 73 pp.

Pruess, K., 1983: Development of the general purpose simulator MULKOM. Earth Sciences Division, annual report 1982, LBL-15500, Lawrence Berkeley Laboratory.

Salera, J.R.M., and O'Sullivan, M.J., 1987: Computer modelling studies of the Tongonan geothermal field. Proceedings of the 9th New Zealand Geothermal Workshop, University of Auckland, 169-177.

Sanchez, D.R., 1993: Application of Cl, B tracers and geoindicators to delineate some production characteristics of Mt. Labo geothermal system, Philippines. UNU G.T.P., Iceland, report 14, 42 pp.

Saw, V.S., 1993: Well MG-8D completion test report. PNOC-EDC, internal report, 18 pp.

Urmeneta, N.N.A., 1993: MG-1RD completion test report. PNOC-EDC, internal report, 9 pp.

Whittome, A.J., and Smith, E.W., 1979: A model of the Tongonan geothermal field. Proceedings of the 1st New Zealand Geothermal Workshop, University of Auckland, part 1, 141-147.